IEEE Access
Multidisciplinary | Rapid Review | Open Access Journal

Received January 17, 2022, accepted February 6, 2022, date of publication February 10, 2022, date of current version February 17, 2022.

Digital Object Identifier 10.1109/ACCESS.2022.3150845

Event-Triggered Diagnostic Observer Design Using the Performance Tradeoff Approach

JINGSONG WU, MINGFANG WU, SHENGFENG WANG, AND AIBING QIU
School of Electrical Engineering, Nantong University, Nantong 226019, China

Corresponding authors: Shengfeng Wang (wangsf@ntu.edu.cn) and Aibing Qiu (aibqiu@ntu.edu.cn)

This work was supported in part by the National Natural Science Foundation of China under Grant 61473159 and Grant U2066203; in part by the Six Talent Peaks Project in Jiangsu Province under Grant XYDXX-091; in part by the Key Program of Science and Technology of Nantong under Grant MS22020030, Grant MS22020022, and Grant JC2020094; and in part by the Natural Science Research Program of Jiangsu Colleges and Universities under Grant 20KJA470002.

ABSTRACT This paper presents an optimal diagnostic observer design scheme to deal with the remote fault detection problem for a local closed-loop system with unknown external disturbances and faults. To utilize limited network shared resources efficiently, an event-triggered generator is employed in the local closed-loop system to determine whether to transmit the current output measurement for fault detection. By constructing the error system that contains event-triggered transmission errors and evaluating the composition of the residual under the constraint of Luenberger conditions, the diagnostic observer which has optional order and flexible structure is designed by the use of factorization techniques to achieve the optimal performance tradeoff between disturbance robustness and fault sensitivity. Next, the inevitable influence of reference input on the residual is taken into account in the residual evaluation to deliver a time-varying threshold. Finally, a vehicle lateral dynamic system is presented to illustrate the validity of the proposed optimal diagnostic observer design scheme.

INDEX TERMS Diagnostic observer, event-triggered system, fault detection, performance tradeoff.

I. INTRODUCTION

As modern engineering systems become larger and more complex, remote monitoring and control have become the norm with the assistance of network communication technology. In these types of modern control systems, there is a high demand in efficiently using the shared network, computing, or energy resources. Given this background, event-triggered techniques have emerged [1]–[3]. Compared with traditional time-triggered techniques, the event-triggered technique can be regarded as an on-demand nonuniform sampling and communication method, which only executes actions when some predefined conditions are satisfied, thereby reducing computational complexity and unnecessary communication and energy consumption. Besides, some elaborate event-triggered mechanisms can improve control performance and detection accuracy [4], [5]. Considering those advantages of the event-triggered technique, various kinds of event-triggered mechanisms such as absolute error, relative error, self-adaptation, self-triggered ones, have been successively proposed to apply to control and estimation of various complex network systems [6]–[9]. Also, some experiments on practical systems such as vehicle platooning and unmanned aerial vehicles were carried out to show the superiority of the event-triggered techniques [10]–[12]. For more details on this topic, please see the survey papers [1], [13].

On the other hand, one of the main purposes of remote monitoring is to promptly discover and diagnosis potential faults in the system so as to take some reasonable remedies. Similar to control and estimation problems, the event-triggered mechanism can also be employed for fault detection. However, due to the use of event-triggered technique, the remote monitoring center will lose some system information and the system characteristics will change, which increase some difficulties to remote fault detection [14], [15]. The research on event-triggered fault detection has received widespread attention in the past few years [16]–[22]. Basically, the existing event-triggered fault detection approaches, from the perspective of design idea, can be divided into two categories: the optimal identification based one and the performance tradeoff based one. The basic idea of the optimal identification based event-triggered fault detection approach is to design a fault detection filter to make the generated residual signal approach the fault by expanding

The associate editor coordinating the review of this manuscript and approving it for publication was Guillermo Valencia-Palomo.

This work is licensed under a Creative Commons Attribution 4.0 License. For more information, see https://creativecommons.org/licenses/by/4.0/

the faulty system and the error system into an augmented system. Under the optimal filtering framework, the event-triggered fault detection problem is easily formulated and handled. Therefore, the optimal identification based method was widely used in various complex network control systems such as Markov jump systems, T-S fuzzy systems and nonlinear networked systems with output quantisation [16]–[18]. However, the method requires the estimation error signal of fault to be robust to all external inputs, which reduces the sensitivity to faults and thus deteriorates the fault detection performance [23]. The performance tradeoff based event-triggered fault detection method considers the fault sensitivity and disturbance robustness simultaneously. By introducing some ratio-type or difference-type performance index and applying some optimization technique, the residual generator is designed to make the residual be robust to disturbances and be sensitive to faults. In [19], a tradeoff approach for event-triggered fault detection was developed under the H_∞/H_∞ performance index. It was also verified that the fault detection performance of the tradeoff based method was much superior to the optimal identification based one. In [20], an optimal event-triggered fault detection filter was designed under the H_i/H_∞ performance index. The generated residual was decoupled from the event-triggered transmission error. Similarly, in [21], the optimal parity space based event-triggered fault detection scheme was developed under the H_2/H_2 performance index. In the framework of nonuniform sampled system, the residual generators in [20], [21] were time-varying whose parameters require online calculation. More recently, by introducing a novel parity vector based event-triggered mechanism, the parity space based event-triggered fault detection was also investigated in [22]. The influence of the event-triggered transmission error on false alarm rate was firstly quantitatively analyzed.

It is worth noting that the residual generators used in the above two event-triggered fault detection approaches are either fault detection filter or parity space based residual generator. The diagnostic observer, as another common form of residual generator, is preferred in practice due to its optional order and flexible structure [23]. It can reduce the online calculation when the reduced order diagnostic observer is adopted and has more design freedoms when the full or higher-order form is adopted. In [24], an optimal diagnostic observer was developed for sampled-data system. In [25], a robust diagnostic observer was developed for nonlinear system by using the logic-dynamic approach. In [26], to detect the incipient fault in the post-fault system, some design freedoms of diagnostic observer were employed to decouple the incipient fault from the adaptive fault tolerant control. In consideration of the advantages of diagnostic observer, it is desirable to develop a performance tradeoff based diagnostic observer for event-triggered systems for fault detection. However, this is indeed a challenging work. The difficulties arise from: (1) making a tradeoff among unknown external disturbances, faults, and event-triggered transmission errors on the residual due to the use of event-triggered technique changes the dynamic of diagnostic observer, (2) coping with more constraints in the optimization problem because the diagnostic observer should satisfy the Luenberger conditions.

In this paper, a tradeoff approach based event-triggered optimal diagnostic observer is developed for event-triggered systems for fault detection. More specifically, the paper provides the following contributions.

1) By evaluating the influences of unknown external disturbances, faults, and event-triggered transmission errors on the residual, the design of diagnostic observer, where a general event-triggered mechanism is used to reduce the communication load, is formulated as an H_∞/H_∞ optimization problem to make a tradeoff between fault sensitivity and disturbance robustness.

2) An event-triggered optimal diagnostic observer with full or higher-order, which has more design freedom, is designed by the use of factorization techniques. And an algorithm is developed to handle the Luenberger constraints.

3) A time-varying threshold that considers the influence of reference input on the residual is constructed by the use of Linear Matrix Inequality (LMI) technique. Also, a vehicle lateral benchmark system is presented to illustrate the validity of the proposed event-triggered optimal diagnostic observer design scheme for fault detection.

The organization of the paper is as follows. Section II presents the system description. The analysis of diagnostic observer dynamic model, the design of optimal diagnostic observer, and the residual evaluation are developed in Section III. Section IV gives an example to verify the validity of the proposed scheme. Section V concludes the paper.

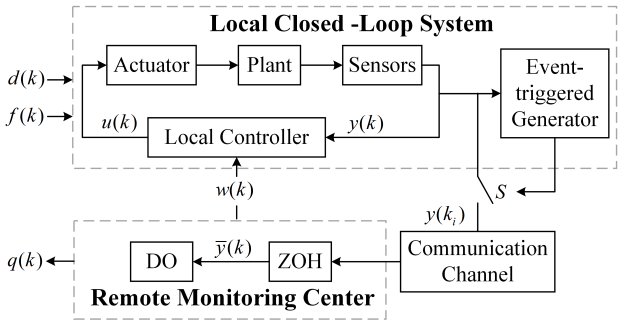

FIGURE 1. The structure of optimal diagnostic observer for an event-triggered system.

II. SYSTEM DESCRIPTION

Consider the following local closed-loop system to be monitored

$$\begin{aligned} x(k+1) &= Ax(k) + B_w w(k) + B_d d(k) + B_f f(k), \\ y(k) &= Cx(k) + D_w w(k) + D_d d(k) + D_f f(k), \end{aligned} \quad (1)$$

where $x(k) \in \mathbb{R}^n$ denotes the state vector, $w(k) \in \mathbb{R}^{n_w}$ denotes the reference input vector, $d(k) \in \mathbb{R}^{n_d}$ denotes the unknown external disturbance vector, $y(k) \in \mathbb{R}^m$ denotes the measured output vector, and $f(k) \in \mathbb{R}^{n_f}$ denotes the

fault vector which may occur in the plant, actuator, or sensor. $A, B_w, B_d, B_f, C, D_w, D_d, D_f$ are system parameter matrices with appropriate dimensions. Moreover, A is assumed to be stable and the pair (A, C) is detectable.

To reduce the communication load from the local closed-loop system to the remote monitoring center, an event-triggered generator is employed, as shown in Fig.1, to decide whether to transmit the current output measurement through the communication channel. More specifically, the event-triggered function is defined as:

$$f\left(e_y(k), \delta, \Omega\right) = e_y^{\mathrm{T}}(k)\Omega e_y(k) - \delta y^{\mathrm{T}}(k)\Omega y(k), \tag{2}$$

where $e_y(k) := y(k_i) - y(k)$ and $y(k_i)$ denotes the transmitted measurement that satisfies the event-triggered condition last time, $\delta \in [0, 1)$ denotes the event-triggered parameter, and $\Omega = M^{\mathrm{T}}M$ is a positive definite weighting matrix to be set. If $f(e_y(k), \delta, \Omega) > 0$, the event-triggered generator closes the switch S and transmits the current output measurement $y(k)$ to the remote monitoring center at time instant k. Otherwise, the output measurement will not be transmitted. Therefore, the next triggering time k_{i+1} can be defined as:

$$k_{i+1} = k_i + \min_{1 \le j \le \tau_{\max}} \left\{ j \mid f\left(e_y(k_i), \delta, \Omega\right) > 0 \right\}, \tag{3}$$

where $e_y(k_i) := y(k_i + j) - y(k_i)$, τ_{max} denotes the max time interval for the event-triggered generator to trigger.

In the remote monitoring center, the received nonuniform measurement $y(k_i)$ is transformed into a uniform one $\bar{y}(k)$ using a zero-order-holder (ZOH), which means $\bar{y}(k) = y(k_i), \forall k \in [k_i, k_{i+1})$. Then define the event-triggered transmission error as $\bar{e}_y(k) := \bar{y}(k) - y(k)$, the inequality will be satisfied as follows

$$\bar{e}_y^{\mathrm{T}}(k)\Omega\bar{e}_y(k) \le \delta y^{\mathrm{T}}(k)\Omega y(k), \forall k \in [k_i, k_{i+1}). \tag{4}$$

Further, the following diagnostic observer (DO) is utilized for the residual generation

$$\begin{aligned} z(k+1) &= Fz(k) + Ow(k) + L\bar{y}(k) \\ \hat{y}(k) &= \bar{N}z(k) + \bar{V}\bar{y}(k) + \bar{Q}w(k) \\ r(k) &= R(k) * (\bar{y}(k) - \hat{y}(k)) \\ &= R(k) * [V\bar{y}(k) - Nz(k) - Qw(k)], \end{aligned} \tag{5}$$

where $z(k) \in \mathbb{R}^s$ denotes the state vector of the diagnostic observer, $\hat{y}(k) \in \mathbb{R}^m$ denotes the estimated output vector, $r(k) \in \mathbb{R}^m$ denotes the residual vector. $R(k) \in \mathbb{R}^{m \times m}$ is the impulse response matrix of a stable linear time-invariant post-filter to be designed. The symbol * denotes convolution. Moreover, the matrix F, O, L, V, N, Q are design parameters of the diagnostic observer, and $\bar{N}, \bar{V}, \bar{Q}$ satisfy $N = \bar{N}, V = I - \bar{V}, Q = \bar{Q}$. The above-mentioned matrices should meet the following Luenberger conditions as shown in Lemma 1.

Lemma 1 ([23, p. 81-82]): Given a matrix $T \in \mathbb{R}^{s \times n}$, the design matrices F, O, L, V, N, Q of the diagnostic observer should satisfy the so-called Luenberger conditions:

$$i.\quad F \text{ is stable}, \tag{6}$$

$$ii.\quad TA - FT = LC,\ O = TB_w - LD_w, \tag{7}$$

$$iii.\quad VC - NT = 0,\quad Q = VD_w. \tag{8}$$

Remark 1: If there is no event-triggered generator in the local closed-loop system, it is the output measurement $y(k)$ that is received by the remote monitoring center. In this case, the above Luenberger equations (7) and (8) can ensure that the residual $r(k)$, under the fault-and-disturbance-free case, will tend to zero for any known reference input $w(k)$, that is $\lim_{k\to\infty} r(k) = 0$, $\forall w(k) \in \mathbb{R}^{n_w}$, $d(k) = f(k) = 0$. Otherwise, if the event-triggered generator is used, the residual $r(k)$ no longer tends to zero because of the event-triggered transmission error $\bar{e}_y(k)$. However, the Luenberger conditions still make the residual $r(k)$ be decoupled from the reference input $w(k)$ as much as possible, which will be analyzed in the Subsection III-A.

Remark 2: Besides the advantages of the flexible structure, the proposed event-triggered diagnostic observer scheme has some other merits when compared with the existing performance based event-triggered fault detection works [19], [20]. The residual generator used in [20] were time-varying systems and all parameters were calculated online at every triggering instant, which obviously requires a high online computation load. In [19], a relative error based event-triggered mechanism was used, while a general event-triggered mechanism (3) is used in this work, which can further reduce the communication load.

III. MAIN RESULTS

In this section, the main results are presented including the analysis of diagnostic observer dynamic model, the design of optimal diagnostic observer, and residual evaluation.

A. THE ANALYSIS OF DIAGNOSTIC OBSERVER DYNAMIC MODEL

Define the estimation error vector $e(k) = Tx(k) - z(k)$, and from (1) and (5) the following error system can be obtained as:

$$\begin{aligned} e(k+1) &= (TA - LC)x(k) + (TB_w - LD_w)\,w(k) \\ &\quad -Fz(k) - Ow(k) + (TB_d - LD_d)\,d(k) \\ &\quad + \left(TB_f - LD_f\right)f(k) - L\bar{e}_y(k), \\ r(k) &= R(k) * \{VCx(k) + (VD_w - Q)w(k) \\ &\quad + VD_d d(k) + VD_f f(k) \\ &\quad + V\bar{e}_y(k) - Nz(k)\}. \end{aligned} \tag{9}$$

Substituting the Luenberger equations (7) and (8) into (9) yields

$$\begin{aligned} e(k+1) &= Fe(k) + (TB_d - LD_d)\,d(k) \\ &\quad + \left(TB_f - LD_f\right)f(k) - L\bar{e}_y(k), \\ r(k) &= R(k) * \{Ne(k) + VD_d d(k) \\ &\quad + VD_f f(k) + V\bar{e}_y(k)\}. \end{aligned} \tag{10}$$

It can be seen from (10) that the residual $r(k)$ appears to be decoupled from the reference input $w(k)$. However, due to the use of the event-triggered generator, the residual $r(k)$ will

be affected by the event-triggered transmission error $\bar{e}_y(k)$. Note that $\bar{e}_y(k)$ is affected by all external inputs including $w(k)$. Therefore, although the Luenberger conditions reduce the influence of $w(k)$ on $r(k)$ as much as possible, the perfect decoupling of $r(k)$ from $w(k)$ will not be achieved.

Taking the Z-transform of (10), the input-output dynamic of the residual generator is obtained as:

$$\begin{aligned} r(z) &= R(z)\left[G_{d,r}(z)d(z)+G_{f,r}(z)f(z)+G_{\bar{e}_y,r}(z)\bar{e}_y(z)\right], \\ G_{d,r}(z) &= VD_d+N(zI-F)^{-1}\left(TB_d-LD_d\right), \\ G_{f,r}(z) &= VD_f+N(zI-F)^{-1}\left(TB_f-LD_f\right), \\ G_{\bar{e}_y,r}(z) &= V-N(zI-F)^{-1}L. \end{aligned} \tag{11}$$

Next, we will analyze the influences of the fault $f(k)$, the unknown external disturbance $d(k)$, and the event-triggered transmission error $\bar{e}_y(k)$ on the residual $r(k)$. Note that the event-triggered transmission error $\bar{e}_y(k)$ is driven by all external inputs, including the reference input $w(k)$, the unknown external disturbance input $d(k)$ and the fault $f(k)$, so its influence on the residual $r(k)$ is essentially reflected in the influences of all external inputs on the residual $r(k)$. Therefore, we first evaluate the influence of the external disturbance $d(k)$ on the residual $r(k)$, and note that the external disturbance $d(k)$ also affects the residual $r(k)$ through the event-triggered transmission error $\bar{e}_y(k)$. In case of fault-free ($f(k) = 0$) and no reference input ($w(k) = 0$), the influence of the unknown external disturbance $d(k)$ on the residual $r(k)$ can be described as:

$$\begin{aligned} &\|r_d(k)\|_2 \\ &= \|r(k)\|_2|_{f=0,w=0} \\ &\le \left\|RG_{d,r}d(k)\right\|_2+\left\|RG_{\bar{e}_y,r}M^{-1}M\bar{e}_y(k)\right\|_2 \\ &\le \left\|RG_{d,r}d(k)\right\|_2+\left\|RG_{\bar{e}_y,r}\right\|_\infty\left\|M^{-1}\right\|_2\left\|M\bar{e}_y(k)\right\|_2. \end{aligned}$$

Then, according to the inequality (4), we have

$$\begin{aligned} &\|r_d(k)\|_2: \\ &= \|r(k)\|_2|_{f=0,w=0} \\ &\le \left\{\left\|RG_{d,r}\right\|_\infty+\varepsilon\gamma_d\left\|RG_{\bar{e}_y,r}\right\|_\infty\right\}\left\|M^{-1}\right\|_2\|M\|_2\|d(k)\|_2 \\ &\le 2\left\|R\begin{bmatrix}G_{d,r} & \varepsilon\gamma_d G_{\bar{e}_y,r}\end{bmatrix}\right\|_\infty\left\|M^{-1}\right\|_2\|M\|_2\|d(k)\|_2, \end{aligned}$$

where $\gamma_d = ||G_d||_\infty$, $G_d(z)=D_d+C(zI-A)^{-1}B_d$, $\varepsilon^2=\delta$.

Similarly, in case of disturbance-free ($d(k) = 0$) and no reference input ($w(k) = 0$), the influence of the fault $f(k)$ on the residual $r(k)$ can be described as:

$$\begin{aligned} &\left\|r_f(k)\right\|_2: \\ &= \|r(k)\|_2|_{d=0,w=0} \\ &\le \left\|RG_{f,r}f(k)\right\|_2+\left\|RG_{\bar{e}_y,r}M^{-1}M\bar{e}_y(k)\right\|_2 \\ &\le \left\{\left\|RG_{f,r}\right\|_\infty+\varepsilon\gamma_f\left\|RG_{\bar{e}_y,r}\right\|_\infty\right\}\left\|M^{-1}\right\|_2\|M\|_2\|f(k)\|_2 \\ &\le 2\left\|R\begin{bmatrix}G_{f,r} & \varepsilon\gamma_f G_{\bar{e}_y,r}\end{bmatrix}\right\|_\infty\left\|M^{-1}\right\|_2\|M\|_2\|f(k)\|_2, \end{aligned}$$

where $\gamma_f = ||G_f||_\infty$, $G_f(z) = D_f + C(zI - A)^{-1}B_f$.

In the design of the residual generator, the residual $r(k)$ should be sensitive to the fault $f(k)$ as much as possible, and meantime, be robust to the external disturbance $d(k)$. In order to make a performance tradeoff between disturbance robustness and fault sensitivity, the following H_∞/H_∞ performance index is optimized

$$\min_{L,R(z)} J(L,R(z)) = \min_{L,R(z)}\frac{\left\|R(z)\begin{bmatrix}G_{d,r}(z) & \varepsilon\gamma_d G_{\bar{e}_y,r}(z)\end{bmatrix}\right\|_\infty}{\left\|R(z)\begin{bmatrix}G_{f,r}(z) & \varepsilon\gamma_f G_{\bar{e}_y,r}(z)\end{bmatrix}\right\|_\infty}. \tag{12}$$

It should be noted that, in (12), the variables to be optimized are only L and $R(z)$. The other parameters ε, γ_d, γ_f are either be chosen or obtained from the known system matrices. In addition, the transfer functions $G_{d,r}(z)$, $G_{\bar{e}_y,r}(z)$, $G_{f,r}(z)$ are related to the design parameters N, F, T, L, V. However, based on the Luenberger condition equations (7) and (8), the matrix F can be determined by T and L, the matrix N can also be determined by V and T. Therefore, as long as T and V are selected, the other design parameters are also be determined.

Further, in order to simplify the residual generator, the post-filter $R(k)$ can be limited as a constant matrix W, the optimization problem is accordingly expressed as:

$$\min_{L,W} J(L,W) = \min_{L,W}\frac{\left\|W\begin{bmatrix}G_{d,r}(z) & \varepsilon\gamma_d G_{\bar{e}_y,r}(z)\end{bmatrix}\right\|_\infty}{\left\|W\begin{bmatrix}G_{f,r}(z) & \varepsilon\gamma_f G_{\bar{e}_y,r}(z)\end{bmatrix}\right\|_\infty}. \tag{13}$$

Remark 3: In the Subsection III-A, we only analyze the influences of the unknown external disturbance $d(k)$, the fault $f(k)$ and its corresponding event-triggered transmission error $\bar{e}_y(k)$ on the residual $r(k)$. The influence of the reference input $w(k)$ on the residual $r(k)$ will be analyzed in the residual evaluation stage since $w(k)$, which is different from $d(k)$ and $f(k)$, is generally known.

B. THE DESIGN OF OPTIMAL DIAGNOSTIC OBSERVER

Before solving the optimization problems (12) and (13), the following two Lemmas are introduced.

Lemma 2 ([19]): Suppose that the discrete Linear Time Invariant system $G(z) = (A, B, C, D)$ has no transmission zeros on the unit circle. Then, $G(z)$ can be decomposed into $G(z) = G_{co}(z)G_{ci}(z)$ by the co-inner-outer factorization technique and the following equations are satisfied

$$\begin{aligned} G_{ci}\left(e^{j\theta}\right)G_{ci}^*\left(e^{j\theta}\right) &= I, \theta\in[0,2\pi], \\ G_{co}^{-1}(z) &= H-HC(zI-(A-LC))^{-1}L, \\ G_{ci}(z) &= HD+HC(zI-(A-LC))^{-1}(B-LD), \\ L &= \left(AXC^{\mathrm{T}}+BD^{\mathrm{T}}\right)\left(CXC^{\mathrm{T}}+DD^{\mathrm{T}}\right)^{-1}, \end{aligned}$$

where X is the stable solution of the discrete time Riccati equation

$$AXA^{\mathrm{T}} - X + BB^{\mathrm{T}} - \left(AXC^{\mathrm{T}} + BD^{\mathrm{T}}\right) \left(CXC^{\mathrm{T}} + DD^{\mathrm{T}}\right)^{-1} \left(CXA^{\mathrm{T}} + DB^{\mathrm{T}}\right) = 0, \quad (14)$$

$G_{ci}^{*}(e^{j\theta})$ is the conjugate transpose of $G_{ci}(e^{j\theta})$, G_{co}^{-1} is the inverse of $G_{co}(z)$, and $H = (CXC^{\mathrm{T}} + DD^{\mathrm{T}})^{-1/2}$.

Lemma 3 ([23, p. 23-24]): Suppose that the discrete Linear Time Invariant system $G(z) = (A, B, C, D)$ is stabilizable and detectable. Let E and L be so that $A+BE$ and $A-LC$ are Hurwitz matrix, and define $\hat{M}(z) = (A - LC, -L, C, I)$ and $\hat{N}(z) = (A-LC, B-LD, C, D)$. Then, we can obtain the Left Coprime Factorization (LCF) of $G(z)$:$G(z) = \hat{M}^{-1}(z)\hat{N}(z)$.

Now, we are in the position to present the design method of the optimal observer gain matrix L and the weighted matrix W.

Theorem 1: The optimal parameters L and W to be designed in the diagnostic observer are

$$\begin{aligned} L_{\mathrm{opt}} &= \left\{TAT^{\diamond}X\left(CT^{\diamond}\right)^{\mathrm{T}} + TB_dD_d^{\mathrm{T}}\right\} \left\{CT^{\diamond}X\left(CT^{\diamond}\right)^{\mathrm{T}} + D_dD_d^{\mathrm{T}} + \delta\gamma_d^2 I\right\}^{-1}, \\ W_{\mathrm{opt}} &= \left\{V\left[CT^{\diamond}X\left(CT^{\diamond}\right)^{\mathrm{T}} + D_dD_d^{\mathrm{T}} + \delta\gamma_d^2 I\right]V^{\mathrm{T}}\right\}^{-1/2}, \end{aligned} \quad (15)$$

where $T^{\diamond}$ denotes the generalized inverse of T, X is the stable solution of the following discrete time Riccati equation

$$\begin{aligned} &(TAT^{\diamond})X(TAT^{\diamond})^{\mathrm{T}} - [TAT^{\diamond}X(CT^{\diamond})^{\mathrm{T}} + TB_dD_d^{\mathrm{T}}] \\ &\quad [CT^{\diamond}X(CT^{\diamond})^{\mathrm{T}} + D_dD_d^{\mathrm{T}} + \delta\gamma_d^2 I]^{-1}[CT^{\diamond}X(TAT^{\diamond})^{\mathrm{T}} \\ &\quad + D_dB_d^{\mathrm{T}}T^{\mathrm{T}}] - X + TB_dB_d^{\mathrm{T}}T^{\mathrm{T}} = 0. \end{aligned} \quad (16)$$

Proof: Define ■

$$\begin{aligned} G_{d\bar{e}_y,r}(z) &= \left[\, G_{d,r}(z) \;\; \varepsilon\gamma_d G_{\bar{e}_y,r}(z) \,\right] \\ &= N(zI - F)^{-1}\left[\, TB_d - LD_d \;\; -\varepsilon\gamma_d L \,\right] \\ &\quad + \left[\, VD_d \;\; \varepsilon\gamma_d V \,\right], \end{aligned} \quad (17)$$

$$\begin{aligned} G_{f\bar{e}_y,r}(z) &= \left[\, G_{f,r}(z) \;\; \varepsilon\gamma_f G_{\bar{e}_y,r}(z) \,\right] \\ &= N(zI - F)^{-1}\left[\, TB_f - LD_f \;\; -\varepsilon\gamma_f L \,\right] \\ &\quad + \left[\, VD_f \;\; \varepsilon\gamma_f V \,\right]. \end{aligned} \quad (18)$$

Then the optimization problem (12) is transformed into

$$\min_{L,R(z)} J(L, R(z)) = \min_{L,R(z)} \frac{\left\|R(z)G_{d\bar{e}_y,r}(z)\right\|_{\infty}}{\left\|R(z)G_{f\bar{e}_y,r}(z)\right\|_{\infty}}. \quad (19)$$

Next, we solve the optimization (19) in two steps. Firstly, assume that the observer gain L is fixed, namely $L = L_{fixed}$. By the use of Lemma 2, $G_{d\bar{e}_y,r}(z)$ can be decomposed into

$$G_{d\bar{e}_y,r}(z) = G_{dco}(z)G_{dci}(z). \quad (20)$$

Let $R(z) = Q(z)G_{dco}^{-1}(z)$, $Q(z) \in \mathcal{RH}_{\infty}$ and substituting it into (20) to obtain

$$\begin{aligned} J(R(z)) &= \frac{\left\|R(z)G_{d\bar{e}_y,r}(z)\right\|_{\infty}}{\left\|R(z)G_{f\bar{e}_y,r}(z)\right\|_{\infty}} \\ &= \frac{\left\|Q(z)G_{dco}^{-1}(z)G_{dco}(z)G_{dci}(z)\right\|_{\infty}}{\left\|Q(z)G_{dco}^{-1}(z)G_{f\bar{e}_y,r}(z)\right\|_{\infty}} \\ &= \frac{\|Q(z)\|_{\infty}}{\left\|Q(z)G_{dco}^{-1}(z)G_{f\bar{e}_y,r}(z)\right\|_{\infty}} \\ &\geq \frac{1}{\left\|G_{dco}^{-1}(z)G_{f\bar{e}_y,r}(z)\right\|_{\infty}}. \end{aligned} \quad (21)$$

It is easy to find that when $Q(z) = I$, the equal sign of the inequality (21) holds and the optimal solution of the above performance index is obtained as:

$$R(z) = G_{dco}^{-1}(z) = H - HN\left(zI - (F - L_0N)\right)^{-1}L_0, \quad (22)$$

where

$$\begin{aligned} L_0 &= \{FXN^{\mathrm{T}} + \left[\, TB_d - L_{fixed}D_d \;\; -\varepsilon\gamma_d L_{fixed} \,\right] \\ &\quad \cdot\left[\, VD_d \;\; \varepsilon\gamma_d V \,\right]^{\mathrm{T}}\} \cdot \{NXN^{\mathrm{T}} + \left[\, VD_d \;\; \varepsilon\gamma_d V \,\right] \\ &\quad \cdot\left[\, VD_d \;\; \varepsilon\gamma_d V \,\right]^{\mathrm{T}}\}^{-1} \\ &= \{FXN^{\mathrm{T}} + (TB_d - L_{fixed}D_d)D_d^{\mathrm{T}}V^{\mathrm{T}} \\ &\quad -\delta\gamma_d^2 L_{fixed}V^{\mathrm{T}}\} \cdot \{NXN^{\mathrm{T}} + VD_dD_d^{\mathrm{T}}V^{\mathrm{T}} \\ &\quad +\delta\gamma_d^2 VV^{\mathrm{T}}\}^{-1}. \end{aligned} \quad (23)$$

Define

$$F = TAT^{\diamond} - L_{fixed}CT^{\diamond}, \quad (24)$$

$$N = VCT^{\diamond}. \quad (25)$$

Then, by introducing (24) and (25) into (23), it is obtained that

$$\begin{aligned} L_0 &= \{(TAT^{\diamond} - L_{fixed}CT^{\diamond})X(VCT^{\diamond})^{\mathrm{T}} \\ &\quad +(TB_d - L_{fixed}D_d)D_d^{\mathrm{T}}V^{\mathrm{T}} - \delta\gamma_d^2 L_{fixed}V^{\mathrm{T}}\} \\ &\quad \cdot\{VCT^{\diamond}X(VCT^{\diamond})^{\mathrm{T}} + VD_dD_d^{\mathrm{T}}V^{\mathrm{T}} + \delta\gamma_d^2 VV^{\mathrm{T}}\}^{-1} \\ &= \{TAT^{\diamond}X(CT^{\diamond})^{\mathrm{T}} + TB_dD_d^{\mathrm{T}}\}\{CT^{\diamond}X(CT^{\diamond})^{\mathrm{T}} \\ &\quad +D_dD_d^{\mathrm{T}} + \delta\gamma_d^2 I\}^{-1}V^{-1} - L_{fixed}V^{-1}, \end{aligned} \quad (26)$$

where X is the stable solution of the discrete time Riccati equation (16).

As can be seen from equation (26), when $L_{fixed} = L_{opt}$, $L_0 = 0$, the corresponding $R(z)$ degenerates into a constant matrix, that is $R(z) = W_{opt}$. At this time, the minimum performance index is

$$\min_{L=L_{opt},R(z)} J(R(z)) = \frac{||W_{opt}G_{d\bar{e}_y,r}(z)|_{L=L_{opt}}||_{\infty}}{||W_{opt}G_{f\bar{e}_y,r}(z)|_{L=L_{opt}}||_{\infty}}. \quad (27)$$

Next, we go into the second step. If $G_{d\bar{e}_y,r}(z)$ and $G_{f\bar{e}_y,r}(z)$ are LCF according to Lemma 3, there will always be a reversible matrix $\hat{M}(z) = I - N(zI - (F - (L_{opt} - L)N))^{-1}(L_{opt} - L)$ such that

$$\begin{aligned} G_{d\bar{e}_y,r}(z) &= \hat{M}^{-1}(z)G_{d\bar{e}_y,r}(z)|_{L=L_{opt}}, \\ G_{f\bar{e}_y,r}(z) &= \hat{M}^{-1}(z)G_{f\bar{e}_y,r}(z)|_{L=L_{opt}}, \end{aligned} \quad (28)$$

where $G_{d\bar{e}_y,r}(z)|_{L=L_{opt}}$ and $G_{f\bar{e}_y,r}(z)|_{L=L_{opt}}$ are derived from the transfer functions $G_{d\bar{e}_y,r}(z)$ and $G_{f\bar{e}_y,r}(z)$ with $L = L_{opt}$, respectively.

Considering that the inequality of performance index function $J(R(z)) \leq J(W)$ will always hold, from (27) and (28), it is obtained that

$$\begin{aligned}
&\min_{L=L_{opt},R(z)} J(R(z)) \\
&= \frac{||W_{opt}G_{d\bar{e}_y,r}(z)|_{L=L_{opt}}||_\infty}{||W_{opt}G_{f\bar{e}_y,r}(z)|_{L=L_{opt}}||_\infty} \\
&= \min_{L=L_{opt},R(z)} \frac{||R(z)G_{d\bar{e}_y,r}(z)|_{L=L_{opt}}||_\infty}{||R(z)G_{f\bar{e}_y,r}(z)|_{L=L_{opt}}||_\infty} \\
&= \min_{L,R(z)} \frac{||R(z)\hat{M}(z)G_{d\bar{e}_y,r}(z)||_\infty}{||R(z)\hat{M}(z)G_{f\bar{e}_y,r}(z)||_\infty} \\
&= \min_{L,\tilde{R}(z)} \frac{||\tilde{R}(z)G_{d\bar{e}_y,r}(z)||_\infty}{||\tilde{R}(z)G_{f\bar{e}_y,r}(z)||_\infty} \\
&\leq \min_{L,W} \frac{||WG_{d\bar{e}_y,r}(z)||_\infty}{||WG_{f\bar{e}_y,r}(z)||_\infty}.
\end{aligned} \tag{29}$$

It can be observed that, when $L = L_{opt}$, $W = W_{opt}$, the equality in (29) holds and the optimal performance is obtained. In addition, it can be seen that (15) is the solution to the two optimization problems (12) and (13). Therefore, Theorem 1 is proved.

Nevertheless, only the observer gain matrix L and the weighted constant matrix W are provided in Theorem 1. Based on this, a complete design of the diagnostic observer is concluded in Algorithm 1.

Algorithm 1 An Optimal Event-Triggered Diagnostic Observer Design Algorithm for Fault Detection

S*tep*1 :	Calculate γ_d and select matrix $T \in \mathbb{R}^{s\times n}$ to calculate $T^\diamond$;
S*tep*2 :	According to Theorem 1, calculate L_{opt} and W_{opt};
S*tep*3 :	According to $F = TAT^\diamond - L_{opt}CT^\diamond$ and $O = TB_w - L_{opt}D_w$, calculate F and O;
S*tep*4 :	Judge the stability of the matrix F. If it is unstable, return to S*tep*1. Otherwise, perform S*tep*5;
S*tep*5 :	Select the matrix V, according to $N = VCT^\diamond$ and $Q = VD_w$, calculate N and Q.

Remark 4: In the conventional design process of the diagnostic observer, it is usually to select the three matrices F, L, W firstly, and then to solve the Sylvester equation $TA-FT = LC$ to obtain T, and finally to calculate the remaining matrices according to the Luenberger equations. Differently, in Algorithm 1, the matrix T is firstly selected and then the observer gain L is obtained from Theorem 1. Further, it should be pointed out that since F and N are set as $F = TAT^\diamond - L_{opt}CT^\diamond$ and $N = VCT^\diamond$, the chosen matrix T in the S*tep*1 must satisfy $T^\diamond T = I$ to guarantee the Luenberger conditions (7) and (8). In other words, the matrix T is with full column rank and the diagnostic observer is a full or higher-order observer. As presented in [23, p. 81], the full or higher order observer can play an important role in the optimization of the fault detection and isolation system.

C. RESIDUAL EVALUATION

In this subsection, the residual $r(k)$ is further evaluated, that is, a test statistics Φ based on the residual and the corresponding threshold are designed to determine whether a fault occurs by the following decision logic

$$\begin{cases} \Phi \leq \Phi_{th} \Rightarrow q(k) = 0, & no\ fault \\ \Phi > \Phi_{th} \Rightarrow q(k) = 1, & a\ fualt\ occurs, \end{cases} \tag{30}$$

where the test statistics Φ is chosen as the root mean square (*RMS*)

$$\Phi = ||r(k)||_{RMS} = \left(\frac{1}{Nc}\sum_{j=1}^{Nc}||r(k+j)||^2\right)^{1/2}$$

with Nc denoting the window time, Φ_{th} denotes the threshold, $q(k)$ denotes the alarm sign.

Usually, the threshold is set as the maximum influence of the external inputs on the residual $r(k)$ except the fault $f(k)$. Recall in the error system (10) that the residual $r(k)$ is driven by the external disturbance $d(k)$ and the event-triggered transmission error $\bar{e}_y(k)$ under fault-free case. Thus, the following augmented system (31) composed of the local closed-loop system (1) and the error system (10) is constructed as:

$$\begin{aligned}
\widehat{x}(k+1) &= \widehat{A}\widehat{x}(k) + \widehat{B}_w w(k) + \widehat{B}_d d(k) + \widehat{L}\bar{e}_y(k), \\
r(k) &= \widehat{C}\widehat{x}(k) + W_{opt}D_d d(k) + W_{opt}\bar{e}_y(k),
\end{aligned} \tag{31}$$

where

$$\begin{aligned}
\widehat{x}(k) &= \begin{bmatrix} x(k) \\ e(k) \end{bmatrix}, \quad \widehat{A} = \begin{bmatrix} A & 0 \\ 0 & F \end{bmatrix}, \ \widehat{B}_w = \begin{bmatrix} B_w \\ 0 \end{bmatrix}, \\
\widehat{B}_d &= \begin{bmatrix} B_d \\ TB_d - L_{opt}D_d \end{bmatrix}, \quad \widehat{L} = \begin{bmatrix} 0 \\ -L_{opt} \end{bmatrix}, \\
\widehat{C} &= \begin{bmatrix} 0 & W_{opt}CT^{-1} \end{bmatrix}.
\end{aligned}$$

Note that the event-triggered transmission error $\bar{e}_y(k)$ is essentially driven by unknown external disturbance $d(k)$ and the reference input $w(k)$, then the threshold can be defined as:

$$\begin{aligned}
\Phi_{th} &= \sup_{f(k)=0,d(k),w(k)} ||r(k)||_{RMS} \\
&= \sup_{f(k)=0,d(k),w(k)} ||r_d(k) + r_w(k)||_{RMS} \\
&\leq \sup_{f(k)=0,d(k),w(k)=0} ||r_d(k)||_{RMS} \\
&\quad + \sup_{f(k)=0,d(k)=0,w(k)} ||r_w(k)||_{RMS},
\end{aligned} \tag{32}$$

where $r_d(k)$, $r_w(k)$ denotes the influences of unknown external disturbance $d(k)$ and the reference input $w(k)$ on the residual $r(k)$ respectively. The computation of the threshold (32) is presented in the following Theorem 2.

Theorem 2: If there are positive matrices $\gamma_1, \gamma_2, \beta_1, \beta_2$ and positive semidefinite matrices P_1, P_2, and the following LMIs are satisfied

$$\Sigma_1 = \begin{bmatrix} \Sigma_1 ME_{11} & \Sigma_1 ME_{12} & \Sigma_1 ME_{13} \\ \Sigma_1 ME_{21} & \Sigma_1 ME_{22} & \Sigma_1 ME_{23} \\ \Sigma_1 ME_{31} & \Sigma_1 ME_{32} & \Sigma_1 ME_{33} \end{bmatrix} \leq 0, \quad (33)$$

$$\Sigma_2 = \begin{bmatrix} \Sigma_2 ME_{11} & \Sigma_2 ME_{12} & \Sigma_2 ME_{13} \\ \Sigma_2 ME_{21} & \Sigma_2 ME_{22} & \Sigma_2 ME_{23} \\ \Sigma_2 ME_{31} & \Sigma_2 ME_{32} & \Sigma_2 ME_{33} \end{bmatrix} \leq 0, \quad (34)$$

where

$$\begin{aligned}
\Sigma_i ME_{11} &:= \widehat{A}^{\mathrm{T}} P_i \widehat{A} - P_i + \widehat{C}^{\mathrm{T}} \widehat{C} + \beta_i \delta \tilde{C}^{\mathrm{T}} \Omega \tilde{C}, \quad i = 1, 2, \\
\Sigma_1 ME_{12} &:= \widehat{A}^{\mathrm{T}} P_1 \widehat{B}_d + \widehat{C}^{\mathrm{T}} W_{opt} D_d + \beta_1 \delta \tilde{C}^{\mathrm{T}} \Omega D_d, \\
\Sigma_2 ME_{12} &:= \widehat{A}^{\mathrm{T}} P_2 \widehat{B}_w + \beta_2 \delta \tilde{C}^{\mathrm{T}} \Omega D_w, \\
\Sigma_i ME_{13} &:= \widehat{A}^{\mathrm{T}} P_i \widehat{L} + \widehat{C}^{\mathrm{T}} W_{opt}, \quad i = 1, 2, \\
\Sigma_1 ME_{21} &:= \widehat{B}_d^{\mathrm{T}} P_1 \widehat{A}^{\mathrm{T}} + D_d^{\mathrm{T}} W_{opt}^{\mathrm{T}} \widehat{C} + \beta_1 \delta D_d^{\mathrm{T}} \Omega \tilde{C}, \\
\Sigma_2 ME_{21} &:= \widehat{B}_w^{\mathrm{T}} P_2 \widehat{A}^{\mathrm{T}} + \beta_2 \delta D_w^{\mathrm{T}} \Omega \tilde{C}, \\
\Sigma_1 ME_{22} &:= \widehat{B}_d^{\mathrm{T}} P_1 \widehat{B}_d^{\mathrm{T}} + (W_{opt} D_d)^{\mathrm{T}} (W_{opt} D_d) \\
&\quad - \gamma_1^2 I + \beta_1 \delta D_d^{\mathrm{T}} \Omega D_d, \\
\Sigma_2 ME_{22} &:= \widehat{B}_w^{\mathrm{T}} P_2 \widehat{B}_w^{\mathrm{T}} - \gamma_2^2 I + \beta_2 \delta D_w^{\mathrm{T}} \Omega D_w, \\
\Sigma_1 ME_{23} &:= \widehat{B}_d^{\mathrm{T}} P_1 \widehat{L} + (W_{opt} D_d)^{\mathrm{T}} W_{opt}, \\
\Sigma_2 ME_{23} &:= \widehat{B}_w^{\mathrm{T}} P_2 \widehat{L}, \\
\Sigma_i ME_{31} &:= \widehat{L}^{\mathrm{T}} P_i \widehat{A} + W_{opt}^{\mathrm{T}} \widehat{C}, \quad i = 1, 2, \\
\Sigma_1 ME_{32} &:= \widehat{L}^{\mathrm{T}} P_1 \widehat{B}_d + W_{opt}^{\mathrm{T}} W_{opt} D_d, \\
\Sigma_2 ME_{32} &:= \widehat{L}^{\mathrm{T}} P_2 \widehat{B}_w, \\
\Sigma_i ME_{33} &:= \widehat{L}^{\mathrm{T}} P_i \widehat{L} + W_{opt}^{\mathrm{T}} W_{opt} - \beta_i \Omega, \quad i = 1, 2, \\
\tilde{C} &= \begin{bmatrix} C & 0 \end{bmatrix}.
\end{aligned}$$

Then the augmented system (31) satisfies the H_∞ performance indices $||r_d(k)||_2 \leq \gamma_1 ||d(k)||_2$ and $||r_w(k)||_{RMS} \leq \gamma_2 ||w(k)||_{RMS}$. At this time, the threshold (32) can be set as:

$$\Phi_{th} = \frac{1}{\sqrt{Nc}} \gamma_{1\min} ||d(k)||_2 + \gamma_{2\min} ||w(k)||_{RMS}, \quad (35)$$

where $\gamma_{1\min} = \min(\gamma_1)$, $\gamma_{2\min} = \min(\gamma_2)$.

Proof: Define the Lyapunov function $\mathrm{V}_1(k) = \widehat{x}^{\mathrm{T}}(k) P_1 \widehat{x}(k)$ and the function

$$\Phi_d = \Delta \mathrm{V}_1(k) + r_d^{\mathrm{T}}(k) r_d(k) - \gamma_1^2 d^{\mathrm{T}}(k) d(k) \quad (36)$$

where $\Delta \mathrm{V}_1(k) = \mathrm{V}_1(k+1) - \mathrm{V}_1(k)$.

If there is no faults and external inputs, it can be obtained from (4) that

$$\begin{aligned}
&\beta_1 \bar{e}_y^{\mathrm{T}}(k) \Omega \bar{e}_y(k) \\
&\leq \beta_1 \delta y^{\mathrm{T}}(k) \Omega y(k) \\
&\leq \beta_1 \delta [x^{\mathrm{T}}(k) C^{\mathrm{T}} + d^{\mathrm{T}}(k) D_d^{\mathrm{T}}] \Omega [C x(k) + D_d d(k)] \\
&\leq \beta_1 \delta [x^{\mathrm{T}}(k) C^{\mathrm{T}} \Omega C x(k) + d^{\mathrm{T}}(k) D_d^{\mathrm{T}} \Omega C x(k) \\
&\quad + x^{\mathrm{T}}(k) C^{\mathrm{T}} \Omega D_d d(k) + d^{\mathrm{T}}(k) D_d^{\mathrm{T}} \Omega D_d d(k)] \\
&\leq \beta_1 \delta [x^{\mathrm{T}}(k) C^{\mathrm{T}} \Omega C x(k) + 2 x^{\mathrm{T}}(k) C^{\mathrm{T}} \Omega D_d d(k) \\
&\quad + d^{\mathrm{T}}(k) D_d^{\mathrm{T}} \Omega D_d d(k)] \\
&\leq \beta_1 \delta [\widehat{x}^{\mathrm{T}}(k) \tilde{C}^{\mathrm{T}} \Omega \tilde{C} \widehat{x}(k) + 2 \widehat{x}^{\mathrm{T}}(k) \tilde{C}^{\mathrm{T}} \Omega D_d d(k) \\
&\quad + d^{\mathrm{T}}(k) D_d^{\mathrm{T}} \Omega D_d d(k)]. \quad (37)
\end{aligned}$$

Substituting (37) into (36) yields

$$\begin{aligned}
\Phi_d &= \Delta \mathrm{V}_1(k) + r_d^{\mathrm{T}}(k) r_d(k) - \gamma_1^2 d^{\mathrm{T}}(k) d(k) \\
&= \widehat{x}^{\mathrm{T}}(k+1) P_1 \widehat{x}(k+1) - \widehat{x}^{\mathrm{T}}(k) P_1 \widehat{x}(k) \\
&\quad + r_d^{\mathrm{T}}(k) r_d(k) - \gamma_1^2 d^{\mathrm{T}}(k) d(k) \\
&\leq \eta_1^{\mathrm{T}}(k) \Sigma_1 \eta_1(k), \quad (38)
\end{aligned}$$

where $\eta_1(k) = [\, \widehat{x}^{\mathrm{T}}(k) \; d^{\mathrm{T}}(k) \; \bar{e}_y^{\mathrm{T}}(k) \,]^{\mathrm{T}}$.

It can be seen from (38) that when $\Sigma_1 \leq 0$ the function $\Phi_d \leq 0$ and $\Sigma_{k=0}^{\infty} \Phi_d(k)$ hold under zero initial conditions. Since $\mathrm{V}_1(k+1) = \widehat{x}^{\mathrm{T}}(k+1) P_1 \widehat{x}(k+1) \geq 0$, we finally obtain the inequality $||r_d(k)||_2 \leq \gamma_1 \parallel d(k)||_2$. Similarly, following the same process as above, by defining Lyapunov function $\mathrm{V}_2(k) = \widehat{x}^{\mathrm{T}}(k) P_2 \widehat{x}(k)$ and $\Phi_w = \Delta \mathrm{V}_2(k) + r_w^{\mathrm{T}}(k) r_w(k) - \gamma_2^2 w^{\mathrm{T}}(k) w(k)$, the inequality $||r_w(k)||_2 \leq \gamma_2 ||w(k)||_2$ will holds under zero initial conditions when $\Sigma_2 \leq 0$. Finally, recall that the relationship between RMS-norm and 2-norm of residual signal satisfies $||r(k)||_{RMS} \leq ||r(k)||_2 / \sqrt{Nc}$. Then, for the external disturbance $d(k)$ that needs to satisfy 2-norm bounded, the inequality $||r_d(k)||_{RMS} \leq ||r_d(k)||_2 / \sqrt{Nc}$ will holds. For reference input $w(k)$ that does not need to meet the 2-norm boundedness, $||r_w(k)||_{RMS} \leq \gamma_2 ||w(k)||_{RMS}$ will holds because the 2-norm gain is also the RMS-norm gain. So (35) can be obtained from (32), Theorem 2 is proved. The algorithm 2 is presented for the residual evaluation for fault detection.

Algorithm 2 Residual Evaluation Algorithm for Fault Detection

*Step*1 :	Set RMS-norm window time Nc, use LMI tool to calculate $\gamma_{1\min}$ and $\gamma_{2\min}$.
*Step*2 :	Calculate $||w(k)||_{RMS}$ and determine the threshold Φ_{th} according to equation (35).
*Step*3 :	Calculate $||r(k)||_{RMS}$. If $\Phi \leq \Phi_{th}$, no fault. Otherwise, a fault occurs.

IV. SIMULATION RESULTS

In this section, a benchmark of vehicle lateral dynamic system, as shown in Fig.2, is utilized to illustrate the effectiveness of the proposed method. By assuming that the vehicle is simplified as a center of gravity and thus can only move in x-axis, y-axis, and yaw around z-axis, the benchmark is called as one-track model which is mostly implemented in personal cars. Let the vehicle side slip angle β and the yaw rate r as the state variables $x = [\beta \; r]^{\mathrm{T}}$, the steering angle δ_L^* as the reference input variable, the lateral acceleration sensor a_y and the yaw rate sensor r as output variables $y = [a_y \; r]^{\mathrm{T}}$. The matrices of the continuous-time one-track model and its

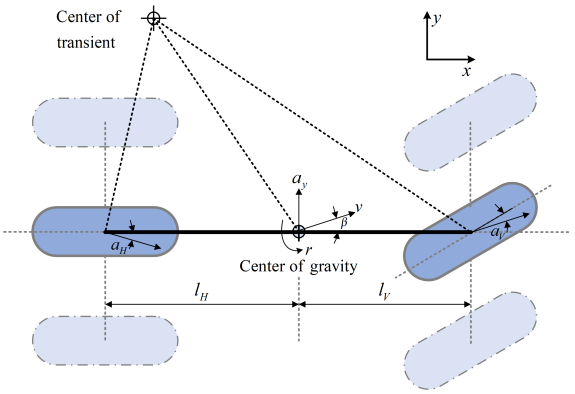

FIGURE 2. The kinematics of one-track model.

measurement model can be obtained as:

$$A = \begin{bmatrix} -\dfrac{C'_{aV} + C_{aH}}{m_g v_{ref}} & \dfrac{l_H C_{aH} - l_V C'_{aV}}{m_g v_{ref}^2} - 1 \\ \dfrac{l_H C_{aH} - l_V C'_{aV}}{I_z} & -\dfrac{l_V^2 C'_{aV} + l_H^2 C_{aH}}{I_z v_{ref}} \end{bmatrix},$$

$$B_w = \begin{bmatrix} \dfrac{C'_{aV}}{m_g v_{ref}} \\ \dfrac{l_V C'_{aV}}{I_z} \end{bmatrix}, \quad D_w = \begin{bmatrix} \frac{C'_{aV}}{m_g} \\ 0 \end{bmatrix},$$

$$C = \begin{bmatrix} -\dfrac{C'_{aV} + C_{aH}}{m_g} & \dfrac{l_H C_{aH} - l_V C'_{aV}}{m_g v_{ref}} \\ 0 & 1 \end{bmatrix}.$$

The detailed explanations of the parameters are summarized in Table 1.

TABLE 1. Parameters of the one-track model.

Physical constant	Value	Unit	Explanation
C_{aH}	179000	N/rad	rear tire cornering stiffness
C'_{aV}	103600	N/rad	front tire cornering stiffness
m_R	1630	kg	rolling sprung mass
m_{NR}	220	kg	non-rolling sprung mass
m_g	m_R+m_{NR}	kg	total mass
v_{ref}	50	km/h	vehicle longitude velocity
l_H	1.53069	m	distance from the center of gravity to the rear axle
l_V	1.52931	m	distance from the center of gravity to the front axle
I_z	3870	$kg{\cdot}m^2$	moment of inertia about the z-axis

By considering the influences of road bank angle, vehicle body roll angle, roll rate, and sensor noises in practice as the external disturbances and discretizing the system with the sampling period 0.1 seconds, the following matrices of the discrete-time vehicle lateral dynamics can be obtained as:

$$A = \begin{bmatrix} 0.6333 & -0.0672 \\ 2.0570 & 0.6082 \end{bmatrix}, \quad B_w = \begin{bmatrix} -0.0653 \\ 3.4462 \end{bmatrix},$$

$$C = \begin{bmatrix} -152.7568 & 1.2493 \\ 0 & 1 \end{bmatrix}, \; D_w = \begin{bmatrix} 56 \\ 0 \end{bmatrix},$$

$$B_d = \begin{bmatrix} 0.1571 & 0.2395 & 0 \\ 0.3977 & 0.5156 & 0 \end{bmatrix}, \; D_d = \begin{bmatrix} 0 & 0 & 1 \\ 0 & 0 & 0 \end{bmatrix}.$$

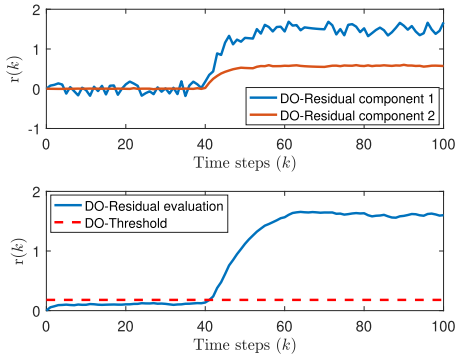

FIGURE 3. Residual of Case 1 with $\Omega = \begin{bmatrix} 1 & 0 \\ 0 & 1 \end{bmatrix}$.

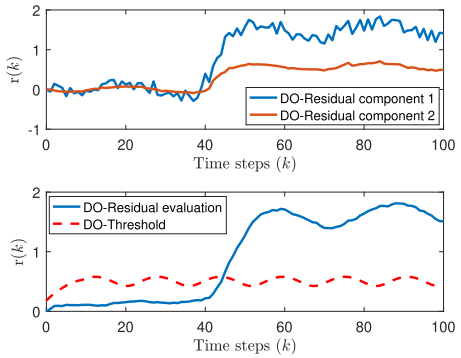

FIGURE 4. Residual of Case 2 with $\Omega = \begin{bmatrix} 1 & 0 \\ 0 & 1 \end{bmatrix}$.

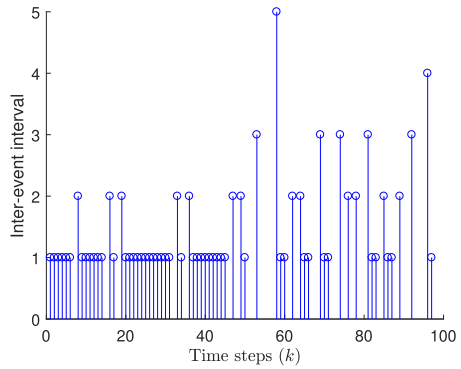

FIGURE 5. Trigger interval of Case 1 with $\Omega = \begin{bmatrix} 1 & 0 \\ 0 & 1 \end{bmatrix}$.

In addition, a typical offset fault is considered in the steering angle sensor, then we can set the fault matrices $B_f = B_w$ and $D_f = D_w$. The triggering parameters are selected as

$\delta = 0.01$, $\Omega = I^{2\times 2}$, $\tau_{\max} = 6$. The window time $Nc = 20$. Now, by selecting the matrices $T = \begin{bmatrix} 1 & 1 & 0 \\ 1 & 0 & 1 \end{bmatrix}^{\mathrm{T}}$, $V = \begin{bmatrix} 1 & 0 \\ 0 & 1 \end{bmatrix}$ and implementing the Algorithm 1, we can obtain $\gamma_d = 90.3499$ and the following design parameters of the optimal diagnostic observer

$$L_{opt} = \begin{bmatrix} -0.0250 & 0.0008 \\ -0.0031 & 0 \\ -0.0220 & 0.0008 \end{bmatrix},$$

$$W_{opt} = \begin{bmatrix} 0.0227 & 0.0013 \\ 0.0013 & 0.1106 \end{bmatrix},$$

$$F = \begin{bmatrix} -0.1877 & -0.9469 & 0.7592 \\ 0.0337 & 0.1309 & -0.0971 \\ -0.2215 & -1.0778 & 0.8563 \end{bmatrix},$$

$$O = \begin{bmatrix} 4.7831 \\ 0.1065 \\ 4.6766 \end{bmatrix}, \quad Q = \begin{bmatrix} 56 \\ 0 \end{bmatrix},$$

$$N = \begin{bmatrix} -50.5025 & -102.2543 & 51.7518 \\ 0.3333 & -0.3333 & 0.6667 \end{bmatrix}.$$

Meanwhile, by implementing the Algorithm 2, we can obtain $\gamma_{1\,\min} = 1.4142$, $\gamma_{2\,\min} = 2.2362$ for threshold calculation.

In the simulation, the fault and the disturbance are assumed to be

$$f(k) = \begin{cases} \pi/12, & k > 40 \\ 0, & elsewhere, \end{cases}$$

$$d(k) = [0.2 \;\; 0.1 \;\; 0.15]^{\mathrm{T}} \cdot \lambda(k),$$

where $\lambda(k)$ denotes the signal uniformly distributed over the interval $[-1, 1]$.

Now, two cases are considered in the simulation. In Case 1, the vehicle is assumed to move in a straight line (namely $w(k) = 0$), the threshold is computed as $\Phi_{th} = 0.18$. In Case 2, the vehicle is moving as a sine trajectory ($w(k) = (\pi/15) * \sin(0.2k)$), and thus the threshold is time-varying. The corresponding fault detection results are shown in Fig.3 and Fig.4 respectively. As shown in Fig.3, the performance tradeoff approach with a time-invariant threshold for fault detection can detect the fault immediately in Case 1. Also, it can be observed from Fig.4 that the coupling between the generated residual and the reference input leads to a time-varying threshold and further results in a small detection delay. Further, as shown in Fig.5 and Fig.6 that the event-triggered mechanism reduced the traffic when compared to the time-triggered mechanism in two cases.

Besides, in order to demonstrate the superiority of the general event-triggered mechanism (3) to the relative error one in [19] in optimizing the frequency of transmission. Note that the general event-triggered mechanism (3) boils down to the relative error event-triggered mechanism in [19] when $\Omega = I^{2\times 2}$ and the constraint that Ω can be any positive definite weighting matrix shows the possibility of changing the performance of the general event-triggered mechanism by selecting a appropriate Ω. Therefore, we reselect $\Omega = \begin{bmatrix} 2 & 3 \\ 3 & 5 \end{bmatrix}$

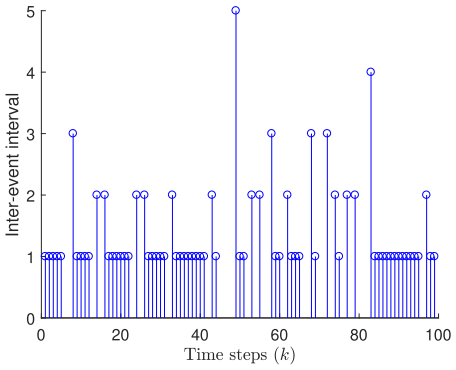

FIGURE 6. Trigger interval of Case 2 with $\Omega = \begin{bmatrix} 1 & 0 \\ 0 & 1 \end{bmatrix}$.

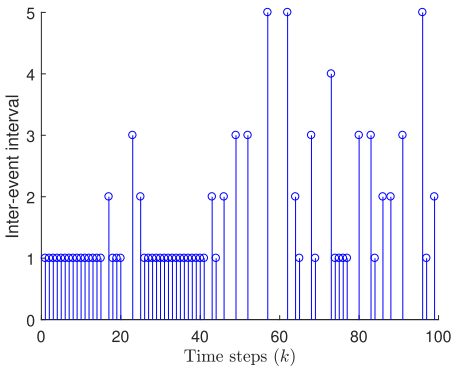

FIGURE 7. Trigger interval of Case 1 with $\Omega = \begin{bmatrix} 2 & 3 \\ 3 & 5 \end{bmatrix}$.

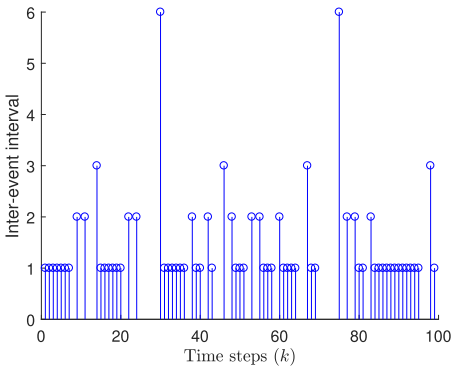

FIGURE 8. Trigger interval of Case 2 with $\Omega = \begin{bmatrix} 2 & 3 \\ 3 & 5 \end{bmatrix}$.

in simulation. As shown in Fig.7, Fig.8, and Table 2, the new Ω can further reduce the traffic in two cases, and the effect is more obvious in Case 1. In addition, it is worth noting that the change of Ω may lead to the change of the detection threshold because Ω is related to the calculation of $\gamma_{1\,\min}$ and $\gamma_{2\,\min}$ in (35).

Further, the residual generation effect and fault detection performance under different event-triggered parameters δ and

TABLE 2. Traffic of different event-triggered parameters.

Ω	Traffic of Case 1	Traffic of Case 2
$\begin{bmatrix} 1 & 0 \\ 0 & 1 \end{bmatrix}$	70	72
$\begin{bmatrix} 2 & 3 \\ 3 & 5 \end{bmatrix}$	63	69

the same event-triggered parameter $\Omega = I^{2\times 2}$ of Case 2 are shown in Fig.9. As can be observed, the threshold is basically unchanged with the increase in the value of the event-triggered parameter δ when $\Omega = I^{2\times 2}$. The coupling between the generated residual and the reference input leads to the detection delay becomes larger and even the fault cannot be detected without $\tau_{\max}$. It means the selection of δ should not only ensure that the LMIs (33) and (34) has a feasible solution, but also make a tradeoff between fault detection performance and communication load.

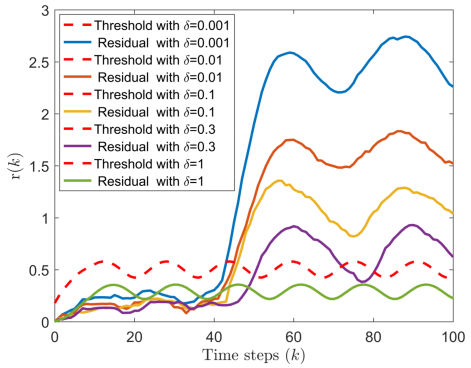

FIGURE 9. Residual of Case 2 with different δ.

V. CONCLUSION

In this paper, we have investigated an event-triggered optimal diagnostic observer for fault detection. Firstly, an H_∞/H_∞ performance index is set by analyzing the composition of the residual to make a tradeoff among unknown external disturbances, faults and event-triggered transmission errors on the residual. Then, an optimal diagnostic observer that considers the event-triggered mechanism is proposed to get a full or higher-order observer under the constraint of the Luenberger conditions. Next, a time-varying threshold including the influence of the reference input on the residual and a test statistics are constructed for fault detection. Finally, simulation results of the vehicle lateral dynamic system are utilized to illustrate the effectiveness of the event-triggered diagnostic observer design using the performance tradeoff approach. In the future, it would be interesting to analyze event-triggered fault detection performance under different event-triggered parameters and utilize the design freedom of the designed diagnostic observer for fault isolation for event-triggered systems. Also, a lower-order diagnostic observer design using the performance tradeoff approach will be investigated. Besides, incipient fault diagnosis [27], [28] under the event-triggered mechanism will be another important research direction for us in the future.

REFERENCES

[1] X.-M. Zhang, Q.-L. Han, and B.-L. Zhang, "An overview and deep investigation on sampled-data-based event-triggered control and filtering for networked systems," *IEEE Trans. Ind. Informat.*, vol. 13, no. 1, pp. 4–16, Feb. 2017.

[2] X. Meng and T. Chen, "Optimal sampling and performance comparison of periodic and event based impulse control," *IEEE Trans. Autom. Control*, vol. 57, no. 12, pp. 3252–3259, Dec. 2012.

[3] F. Forni, S. Galeani, D. Nešić, and L. Zaccarian, "Event-triggered transmission for linear control over communication channels," *Automatica*, vol. 50, no. 2, pp. 490–498, 2014.

[4] M. Donkers and W. Heemels, "Output-based event-triggered control with guaranteed L_∞-gain and improved and decentralized event-triggering," *IEEE Trans. Control Netw. Syst.*, vol. 57, no. 6, pp. 1362–1376, Jun. 2011.

[5] L. Ding, Q. L. Han, X. Ge, and X.-M. Zhang, "An overview of recent advances in event-triggered consensus of multiagent systems," *IEEE Trans. Cybern.*, vol. 48, no. 4, pp. 1110–1123, Apr. 2017.

[6] Y.-L. Wang, C.-C. Lim, and P. Shi, "Adaptively adjusted event-triggering mechanism on fault detection for networked control systems," *IEEE Trans. Cybern.*, vol. 47, no. 8, pp. 2299–2311, Aug. 2017.

[7] T. Zhang, H. Yu, and F. Hao, "A novel distributed event-triggered control with time-varying thresholds," *J. Franklin Inst.*, vol. 357, no. 7, pp. 4132–4153, May 2020.

[8] G. Zong, H. Ren, and H. Reza Karimi, "Event-triggered communication and annular finite-time H_∞ filtering for networked switched systems," *IEEE Trans. Cybern.*, vol. 51, no. 1, pp. 309–317, Jan. 2021.

[9] J. Qiu, K. Sun, T. Wang, and H. Gao, "Observer-based fuzzy adaptive event-triggered control for pure-feedback nonlinear systems with prescribed performance," *IEEE Trans. Fuzzy Syst.*, vol. 27, no. 11, pp. 2152–2162, Dec. 2019.

[10] G. Wu, G. Chen, H. Zhang, and C. Huang, "Fully distributed event-triggered vehicular platooning with actuator uncertainties," *IEEE Trans. Veh. Technol.*, vol. 70, no. 7, pp. 6601–6612, Jul. 2021.

[11] Z. Wu, J. Xiong, and M. Xie, "A switching method to event-triggered output feedback control for unmanned aerial vehicles over cognitive radio networks," *IEEE Trans. Syst., Man, Cybern. Syst.*, vol. 51, no. 12, pp. 7530–7541, Dec. 2021.

[12] V. S. Dolk, J. Ploeg, and W. P. M. H. Heemels, "Event-triggered control for string-stable vehicle platooning," *IEEE Trans. Intell. Transp. Syst.*, vol. 18, no. 12, pp. 3486–3500, Dec. 2017.

[13] W. P. M. H. Heemels, K. H. Johansson, and P. Tabuada, "An introduction to event-triggered and self-triggered control," in *Proc. IEEE 51st Annu. Conf. Decision Control (CDC)*, Dec. 2012, pp. 3270–3285.

[14] A. Qiu, A. W. Al-Dabbagh, H. Yu, and T. Chen, "A design framework for event-triggered active fault-tolerant control systems," *Int. J. Control*, vol. 94, no. 9, pp. 2508–2519, Sep. 2021.

[15] A. Qiu, J. Gu, C. Wen, and J. Zhang, "Self-triggered fault estimation and fault tolerant control for networked control systems," *Neurocomputing*, vol. 272, pp. 629–637, Jan. 2018.

[16] T. Wu, F. Li, C. Yang, and W. Gui, "Event-based fault detection filtering for complex networked jump systems," *IEEE/ASME Trans. Mechatronics*, vol. 23, no. 2, pp. 497–505, Apr. 2017.

[17] X. Su, F. Xia, L. Wu, and C. L. P. Chen, "Event-triggered fault detector and controller coordinated design of fuzzy systems," *IEEE Trans. Fuzzy Syst.*, vol. 26, no. 4, pp. 2004–2016, Aug. 2018.

[18] Y. Pan and G.-H. Yang, "Event-triggered fault detection filter design for nonlinear networked systems," *IEEE Trans. Syst., Man, Cybern. Syst.*, vol. 48, no. 11, pp. 1851–1862, Nov. 2018.

[19] A. Qiu, A. W. Al-Dabbagh, and T. Chen, "A tradeoff approach for optimal event-triggered fault detection," *IEEE Trans. Ind. Electron.*, vol. 66, no. 3, pp. 2111–2121, Mar. 2019.

[20] M. Zhong, S. X. Ding, D. Zhou, and X. He, "An H_i/H_∞ optimization approach to event-triggered fault detection for linear discrete time systems," *IEEE Trans. Autom. Control*, vol. 65, no. 10, pp. 4464–4471, Oct. 2020.
[21] M. Zhong, X. Du, Y. Song, T. Xue, and S. X. Ding, "Event-triggered parity space approach to fault detection for linear discrete-time systems," *IEEE Trans. Syst., Man, Cybern. Syst.*, early access, Aug. 25, 2021, doi: 10.1109/TSMC.2021.3103816.
[22] A. Qiu, X. Ji, and S. Wang, "Parity space-based optimal event-triggered fault detection," *IET Control Theory Appl.*, vol. 15, no. 5, pp. 737–748, Sep. 2021.
[23] S. X. Ding, *Model-based Fault Diagnosis Techniques: Design Schemes, Algorithms, Tools, 2nd ed.* London, U.K.: Springer-Verlag, 2013.
[24] A. Qiu, C. Wen, and B. Jiang, "Optimal diagnostic observer for sampled-data systems," *J. Control Theory Appl.*, vol. 27, no. 8, pp. 979–984, 2010.
[25] A. N. Zhirabok, A. E. Shumskii, S. P. Solyanik, and A. Y. Suvorov, "Design of nonlinear robust diagnostic observers," *Autom. Remote Control.*, vol. 78, no. 9, pp. 1572–1584, Sep. 2017.
[26] W. Chen and F. N. Chowdhury, "Analysis and detection of incipient faults in post-fault systems subject to adaptive fault-tolerant control," *Int. J. Adapt. Control Signal Process.*, vol. 22, no. 9, pp. 815–832, Nov. 2008.
[27] Y. Wu, B. Jiang, and Y. Wang, "Incipient winding fault detection and diagnosis for squirrel-cage induction motors equipped on CRH trains," *ISA Trans.*, vol. 99, pp. 488–495, Apr. 2020.
[28] Y. Wu, B. Jiang, and N. Lu, "A descriptor system approach for estimation of incipient faults with application to high-speed railway traction devices," *IEEE Trans. Syst., Man, Cybern. Syst.*, vol. 49, no. 10, pp. 2108–2118, Oct. 2019.

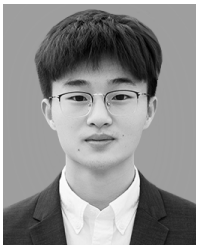

JINGSONG WU received the B.S. degree in building electricity and intelligence from Nantong University, Nantong, China, in 2020, where he is currently pursuing the M.S. degree in control theory and control engineering. His research interests include fault detection and diagnosis for event-triggered systems.

MINGFANG WU received the B.S. degree in electrical engineering and intelligent control from Nantong University, Nantong, China, in 2019, where she is currently pursuing the M.S. degree in control theory and control engineering. Her research interests include fault detection and diagnosis and their applications in the power systems.

SHENGFENG WANG received the M.S. degree in systems engineering from the Nanjing University of Science and Technology, Nanjing, China, in 2004. He is currently a Lecturer with the School of Electrical Engineering, Nantong University. His research interests include fault diagnosis, fault tolerant control, and their applications in the power systems.

AIBING QIU received the Ph.D. degree in control theory and control engineering from the Nanjing University of Aeronautics and Astronautics, Nanjing, China, in 2010. He is currently a Professor with the School of Electrical Engineering, Nantong University. His research interests include fault diagnosis, fault tolerant control, and their applications in the smart building and the smart grid.